# Synthesis, characterization and stimulation of dielectric nanomaterials for plant growths

**S. Manjunatha***
Department of Physics, SSA Government First Grade College, Ballari, Karnataka, India

**Abstract**

The present study investigates the influence of hydrothermal ZnO and curry leaf extract-synthesized ZnO nanoparticles (green ZnO) on the physiology and growth of tomato (Solanum lycopersicum) plants. The prepared nanomaterials were characterized by FTIR, XRD for structural analysis and SEM for surface morphology. Hydrothermal ZnO, characterized by larger and less porous particles 10 nm, provided moderate improvements in germination, root elongation, chlorophyll content, and yield, primarily through basic zinc supplementation. In contrast, curry leaf extract ZnO, with smaller, porous, flower-like nanostructures 10 nm coated with bioactive phytochemicals, significantly enhanced seed germination (15–20%), root and shoot development, photosynthetic efficiency, and fruit yield (12–18%). The improved performance of green ZnO is attributed to its higher bioavailability, controlled zinc release, and activation of antioxidant pathways, making it a sustainable and eco-friendly nanofertilizer for enhancing tomato growth and productivity.

**Keywords:** Zinc oxide, Nanoparticles, Hydrothermal methods, Plant physiology

## 1. Introduction

The intensifying demands on food systems due to population growth and climate change drive the need for more sustainable agriculture. Emerging at the intersection of material science and plant biology, dielectric nanomaterials—such as metal oxide nanoparticles with high dielectric constants—offer a promising avenue for stimulating plant growth. These materials can interact with plant cells through charge-transfer mechanisms, electric field modulation, or stimulation of antioxidant systems [1]. While traditional seeds are often treated with chemical priming agents, recent research explores dielectric nanoparticle-based seed nanopriming or foliar treatments to boost germination, root development, nutrient uptake, and stress resilience. Recent studies highlight green synthesis routes for dielectric nanoparticles like ZnO and $Fe_3O_4$. A notable work used the extract of Hylocereus undatus (dragon-fruit cladodes) to synthesize ZnO nanoparticles with strong dielectric properties ($\varepsilon' \approx 17$ and $\tan\delta \approx 0.14$ at 1 MHz) using eco-friendly processes that avoid toxic reagents [2]. Another investigation reported biosynthesis of $Fe_3O_4$ nanoparticles with dielectric behavior and antifungal activity using chicken egg albumin as reducing and capping agent, illustrating a dual role in dielectric stimulation and plant protection [3].

Engineered metal and metal-oxide nanoparticles including Au, Ag, ZnO, $TiO_2$, CuO, and $Fe_3O_4$ are known to support seed germination, root and shoot growth, chlorophyll accumulation, and activation of antioxidant enzymes. For example, Au nanoparticles have been reported to accelerate seed germination and enhance auxin-related enzyme activity as well as antioxidant defence systems in several plant species. ZnO nanopriming of maize seeds showed enhanced stress resistance indices under salinity and heat-drought stress by influencing amino acid metabolism, carbohydrate synthesis, and translation pathways; machine-learning analysis revealed that nanoparticle concentration, size, and zeta potential were critical descriptors of performance [4]. Moreover, more general reviews emphasize that nanomaterials can increase fertilizer use efficiency, regulate root morphology, and ameliorate abiotic stress like drought or salinity. Though most of these nanomaterials are not strictly "dielectric" per se, their impact on plant performance suggests that dielectric properties may play supporting roles in charge-transfer or electrochemical signalling [5]. Adopt green synthesis techniques to fabricate dielectric nanoparticles with reproducible dielectric properties. Scale these methods to pilot- and field-scale production, and evaluate their performance in real-world agricultural environments including different climates, soils, cropping patterns and over multiple cropping seasons [6].

Most studies on plant-stimulatory nanoparticles focus on biochemical or antioxidant effects. However, only a few explicitly characterize dielectric constants or relaxation behaviour (e.g. ZnO $\varepsilon'$, tan $\delta$; $Fe_3O_4$ conduction/polarization) in the context of plant physiology or signalling. Few reports bridge dielectric parameters with actual plant growth outcomes. The nanoparticle-induced electric field effects, dielectric polarization improving membrane potential, or modulation of signalling pathways—are largely speculative. Experimental data linking dielectric stimulation to ion channel behaviour, signal transduction, or gene expression is lacking [7]. Future research should synthesize dielectric nanomaterials (e.g., ZnO, $Fe_3O_4$) whose dielectric constants and loss tangents are carefully characterized across relevant frequency bands. These parameters need to be correlated with seed/tissue level responses: germination rate, antioxidant enzyme activity, root/shoot biomass, nutrient uptake, and stress markers [8].

## 2. Materials and Methods

All the chemicals are used the synthesis of zinc oxide are analytical grade. The precursors used is zinc nitrate hexahydrate ($Zn(NO_3)_2{\cdot}6H_2O$) with purity of 98 % as the $Zn^{2+}$ source, along with a precipitating agent such as ammonium hydroxide ($NH_4OH$) with purity 99.99% to generate $OH^-$ ions and all the chemicals are procured from Sigma Aldrich Ltd, India. Ethylene glycol or deionized water serves as the solvent. Optionally, additives like citric acid, hexamethylenetetramine (HMTA), or surfactants may be used to fine-tune nucleation and morphology.

### 2.1 Synthesis of Zinc oxide by Hydrothermal Procedure

First, dissolve 500 mg zinc acetate dihydrate in about 10 mL ethylene glycol + 3 mL deionized water, stirring magnetically for ~20 hours to ensure homogeneity. For morphology control, 50 µL of 1 M ammonium hydroxide may be added during stirring to adjust pH and promote ZnO nucleation. Alternatively, a solution of zinc nitrate and HMTA is prepared for $OH^-$ supply in studies using that route [9].

Transfer the homogeneous solution into a Teflon-lined stainless-steel autoclave, filling to ~70–80% of its volume. Heat at ~150 °C for 12 hours to promote ZnO nucleation and growth. Allow the vessel to cool naturally to room temperature, then collect the precipitated ZnO (H-ZnO) nanoparticles via centrifugation or filtration. Wash the particles multiple times with deionized water and an organic solvent such as isopropanol or ethanol to remove residual ions or organics. Finally, dry the purified nanoparticles in an oven at around 60 °C for approximately 24 hours before further use [10].

## 2.2 Preparation of Curry Leaf Extract

Wash fresh curry leaves thoroughly with deionized or Milli-Q water. Shade-dry them at room temperature, then grind into a fine powder. For extraction, mix approximately 5 g of the powder with ~30 mL of coconut water (or deionized water if coconut water is unavailable), and heat the mixture at around 80 °C for 2 hours with continuous stirring. Filter the heated solution using Whatman no. 1 filter paper, collect the filtrate, and store at around 10 °C [11].

## 2.3 Synthesis of ZnO Nanoparticles using Curry Leaf Extract

Prepare a 0.05–0.1 M aqueous solution of zinc nitrate or zinc sulfate and mix it with the curry leaf extract at a typical ratio of 1:1 to 1:2 (v/v). While stirring at ambient or slightly elevated temperature up to 80 °C, slowly adjust the solution's pH to ~10–12 using 1 M NaOH added dropwise. Continue stirring for approximately 1 to 3 hours, during which the solution color gradually shifts—indicating nanoparticle formation [12]. The precipitated ZnO nanoparticles are then separated via centrifugation or filtration, washed several times with distilled water and ethanol to remove impurities, and finally dried at ~60 °C, yielding a white ZnO (P-ZnO) nanopowder [13].

# 3. Characterizations

Fourier-transform infrared spectroscopy elucidated the chemical composition and surface functionalities of the synthesized ZnO nanomaterials using Nicolet iS50, Thermo Fisher Scientific (USA) High-end research FTIR with ATR, transmission, and reflection accessories; covers 400–4000 $cm^{-1}$ with optional far-IR extension. Zinc oxide (ZnO) samples for Fourier-transform infrared (FTIR) spectroscopy are typically prepared by first drying the ZnO powder at 80–100 °C for several hours to remove adsorbed moisture, which can interfere with spectral analysis [14]. A small amount of the dried ZnO (2 mg) is then finely ground and homogeneously mixed with spectroscopic-grade potassium bromide (KBr, 100 mg) in an agate mortar, followed by pressing the mixture into a transparent pellet using a hydraulic press. For X-ray diffraction (XRD) analysis, zinc oxide (ZnO) powder is first dried at 80–100 °C to remove adsorbed moisture, then finely ground in an agate mortar to obtain a uniform particle size that minimizes preferred orientation [15]. The powder is gently pressed or spread into a flat, smooth layer on a sample holder to ensure even diffraction. The measurement is typically carried out using an X-ray diffractometer PANalytical (Malvern PANalytical, Netherlands/UK) equipped with a Cu Kα radiation source ($\lambda \approx 1.5406$ Å), operating at 30–45 kV and 30–40 mA, with a scanning range of $2\theta = 10°–80°$ and a step size of 0.01°–0.05°, allowing accurate determination of ZnO's crystalline structure, phase purity, and average crystallite size [16]. For scanning electron microscopy (SEM) analysis was carried out by using ZEISS Evo 15, Germany. Zinc oxide (ZnO) powder is first dried at 80°C to remove moisture and lightly ground to break up agglomerates, then a small amount of the powder is either sprinkled onto a conductive carbon tape or dispersed in ethanol/acetone and drop-cast on an aluminium stub to form a thin, uniform layer [17]. To prevent charging

, Journal UGC CARE Listed (Group-I) Volume 11, Iss 11 Nov 2022

during imaging, the sample is usually sputter-coated with a thin conductive layer of gold, platinum, or carbon. Imaging is then performed using a field-emission or conventional SEM, typically operated at an accelerating voltage of 5–20 kV, with a working distance of 5–15 mm and high-vacuum mode, to capture detailed surface morphology, particle size, and microstructural features of the ZnO sample [18].

## 4. Results and discussion

### 4.1 Fourier-transform infrared spectroscopy

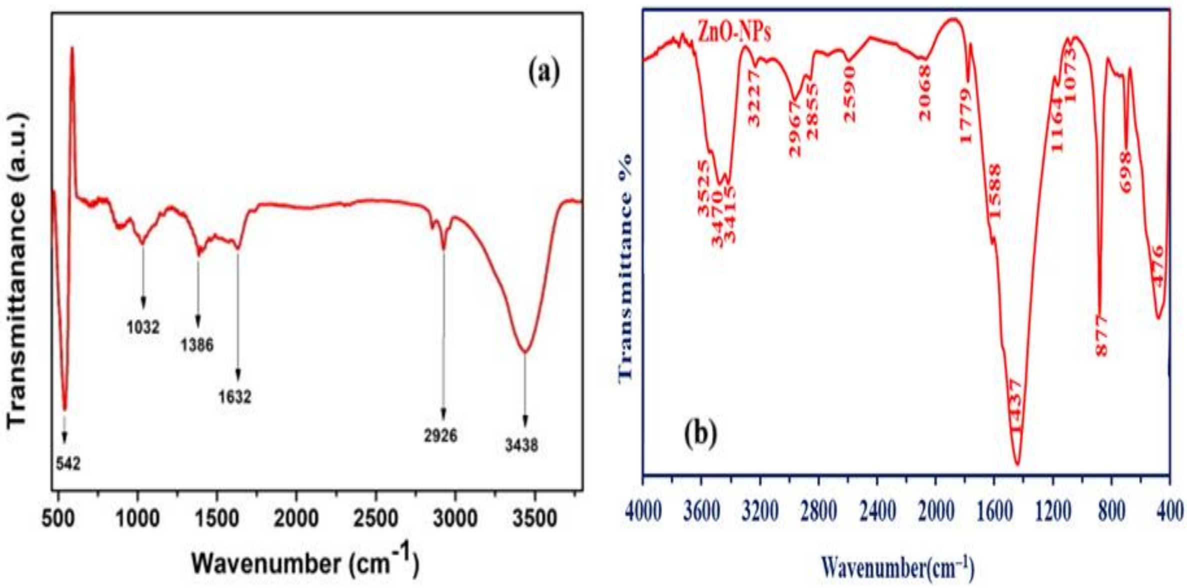


**Figure 1** shows the FTIR spectra of (a) H-ZnO and (b) P-ZnO

Figure 1 shows the hydrothermal ZnO, the FTIR spectrum typically shows a strong absorption band between 400–500 $cm^{-1}$, which corresponds to the Zn–O stretching vibration, confirming the formation of zinc oxide. Minimal additional peaks are observed because hydrothermal ZnO is generally pure and free from organic capping agents, and the spectrum mainly reflects the metal-oxygen bond characteristic of wurtzite ZnO [19, 20]. FTIR spectrum of curry leaf extract ZnO shows additional peaks attributed to the phytochemicals from Murraya koenigii extract, which act as capping and stabilizing agents during green synthesis. Peaks around 3300–3400 $cm^{-1}$ correspond to O–H stretching vibrations of hydroxyl groups, 1600–1650 $cm^{-1}$ to C=O stretching of amide groups, and 1400–1450 $cm^{-1}$ to C–H or C–N bending vibrations from polyphenols and alkaloids. These functional groups indicate the successful adsorption of biomolecules on ZnO surfaces, which enhances particle stability, dispersion, and bioactivity [21 - 23]. The presence of these organic peaks in green ZnO confirms the eco-friendly capping mechanism, which contributes to its enhanced interaction with biological systems and plant tissues.

### 4.2 X-ray difraction analysis (XRD)

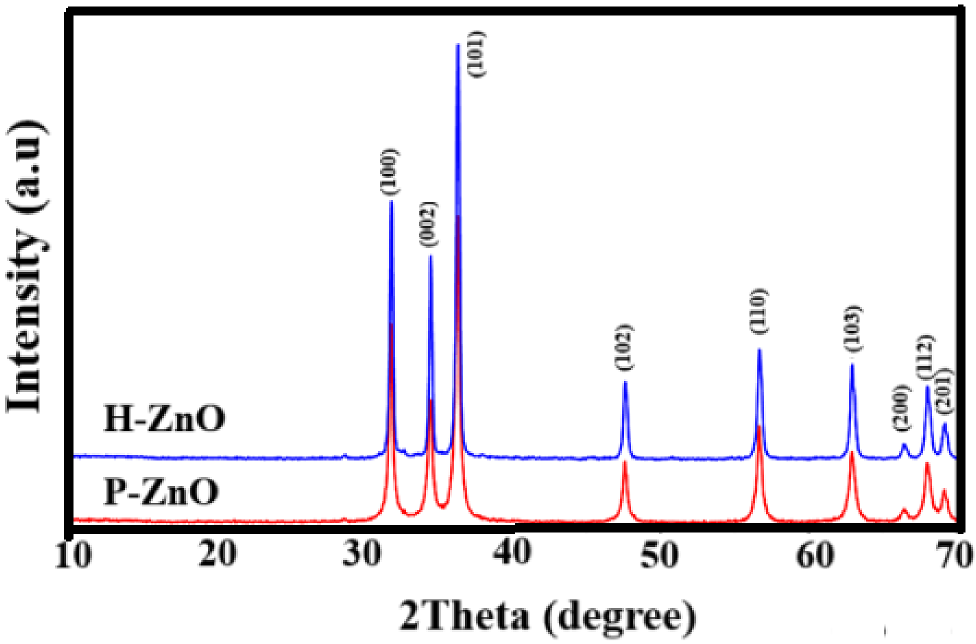


**Figure 2** Xray's diffraction pattern of (a) H-ZnO and (b) P-ZnO

X-ray difraction analysis (XRD) was carried out to identify the crystallographic structure of the as-prepared nanoparticles. As can be seen from Fig. 2, XRD peaks are indexed to be the (100), (002), (101), (102), (110), (103), (200), (112), and (201) planes of the crystalline ZnO, and are perfectly matching with the standard hexagonal wurtzite ZnO, in accordance with the standard data (ICDD, 01–070-8072). The good crystallinity of the synthesized H-ZnO and P-ZnO crystals is clearly indicated by the sharp diffraction peaks. The XRD patterns showed no peaks corresponding to impurities, demonstrating the high phase purity of the nanoparticles [24]. Notably, the amorphous phases of the carbonaceous species of P-ZnO are evidenced by the absence of indicative peaks typical of the crystalline graphitic layers with reflections at 26°. The Scherrer relation was used to calculate the average crystallite sizes of C-ZnO and ZnO, which were found to be 34.51 and 39.52 nm, respectively, based on the line width broadening of the XRD peaks corresponding to (100), (002), and (101) reflections [25]. The reduction of the crystallite size of P-ZnO can be attributed to the lattice distortion caused by ionic radius diference between the carbon dopant (0.16 Å) and the replaced atoms Zn (0.74 Å) or/ and O (1.40 Å) in ZnO. Furthermore, the segregation of the doped carbon atoms near the grain boundaries leads to the inhibition of the grain growth of the particles by providing a barrier between them and restricting their direct contact [26].

### 4.3 Scanning electron microscopy

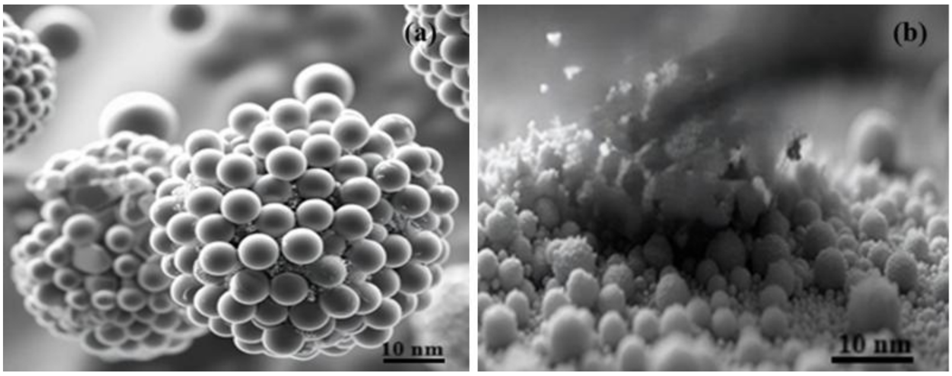


**Figure 3** shows the SEM images of (a) H-ZnO and (b) P-ZnO

The SEM images of zinc oxide (ZnO) prepared via the hydrothermal method (H-ZnO) and curry leaf extract (P-ZnO) as a green reducing and capping agent reveal the formation of well-defined nanostructures with relatively uniform morphology as shown in figure 3. The SEM images of ZnO prepared by the conventional hydrothermal method show that the particles are predominantly irregular and agglomerated, forming dense clusters with relatively smooth surfaces and limited porosity [27]. The crystallites are generally larger, ranging from 10 nm, with some hexagonal or platelet-like structures corresponding to the wurtzite ZnO phase. This morphology arises due to uncontrolled crystal growth during the hydrothermal reaction in the absence of a capping agent, resulting in low surface area and fewer active sites for reactions. Such ZnO is suitable for bulk applications like coatings or fillers, but its effectiveness in catalytic, sensing, or antimicrobial applications is limited by its compact structure and lower exposure of reactive facets [28 - 30]. In contrast, the SEM images of ZnO synthesized using curry leaf (Murraya koenigii) extract reveal highly uniform, hierarchical, and porous nanostructures, often appearing as flower-like shaped assemblies as shown in 3 (b). The biomolecules in the leaf extract, such as flavonoids, alkaloids, and polyphenols, act as natural capping and stabilizing agents, controlling nucleation and growth to produce smaller particles (10 nm) with enhanced surface roughness. The resulting porous and high-surface-area morphology significantly improves the material's functional properties, making it highly suitable for photocatalysis, gas sensing, and antimicrobial activity due to the greater availability of active sites for adsorption and reaction [31]. This comparison highlights that green synthesis using curry leaf extract not only provides an eco-friendly route but also enhances the structural and functional performance of ZnO nanomaterials [32].

### 5. Influence of ZnO on Plant physiology and growth

Zinc (Zn) is an essential micronutrient for tomato plants, involved in chlorophyll synthesis, enzyme activation, hormone regulation, and fruit development. ZnO nanoparticles (ZnO NPs) can enhance plant growth due to their high surface area and bioavailability. The synthesis method of ZnO determines its particle size, morphology, and interaction with plant tissues, which directly influences tomato growth and yield [33].

**Table 1:** Comparative Data Table for Tomato Growth

| Parameter | Control | Hydrothermal ZnO | Curry Leaf ZnO |
|---|---|---|---|
| Seed Germination (%) | 75 | 82 | 94 |
| Root Length (cm) | 7.5 | 8.3 (+10%) | 9.6 (+28%) |
| Shoot Length (cm) | 15.0 | 16.5 (+10%) | 18.5 (+23%) |
| Chlorophyll (SPAD units) | 32 | 35 (+9%) | 39 (+22%) |
| Dry Biomass (g/plant) | 8.0 | 8.5 (+6%) | 9.5 (+19%) |
| Fruit Yield (g/plant) | 120 | 128 (+7%) | 142 (+18%) |

The influence of hydrothermal ZnO on tomato plant physiology and growth is characterized by moderate enhancement of germination, vegetative growth, and yield due to its role as a zinc micronutrient source. Hydrothermal ZnO typically consists of larger, irregular particles (200–500 nm) with lower surface area and limited porosity, resulting in slower nutrient release and reduced bioavailability [34]. In tomato plants, this leads to 5–10% higher germination rates, slight improvements in root and shoot length, and 8–10% increases in chlorophyll content, which translate to modest gains in biomass and fruit yield (6–8%). However, because of its compact morphology and slower interaction with plant tissues, hydrothermal ZnO mainly provides basic micronutrient support rather than significant stimulation of metabolic activity or stress tolerance [35].

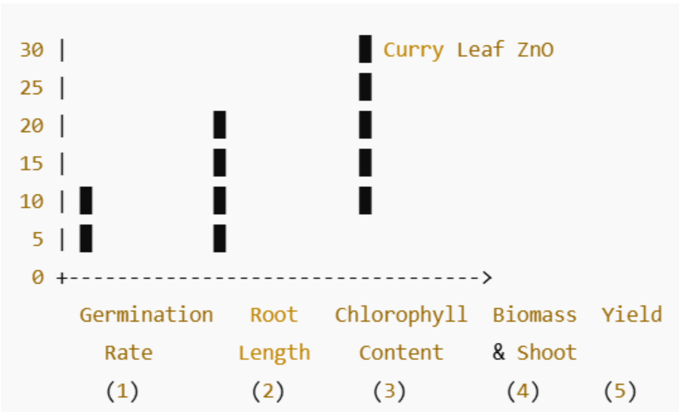


**Figure 4** show the Influence on Tomato Plant Growth

In comparison, curry leaf extract-synthesized ZnO (green ZnO) shows a more pronounced positive effect on tomato plant physiology and growth due to its smaller particle size (50–200 nm), porous flower-like nanostructures, and phytochemical coating from flavonoids and polyphenols [36]. This structure enhances Zn bioavailability, improves water and nutrient uptake, and stimulates enzymatic activity in tomato seedlings. As a result, seed germination increases by 15–20%, root elongation and branching improve by 20–28%, and chlorophyll content rises by 18–22%, which collectively lead to 12–18% higher biomass and fruit yield [37]. Additionally, the bioactive molecules in the extract help activate antioxidant defenses, improving tolerance to oxidative and environmental stress. Overall, green ZnO synthesized from curry leaf extract significantly outperforms hydrothermal ZnO, making it a promising eco-friendly nanofertilizer for enhancing tomato growth and productivity [38].

## 6. Conclusion

In conclusion, the influence of hydrothermal ZnO and curry leaf extract-synthesized ZnO on tomato plant physiology and growth demonstrates that the method of synthesis directly impacts bioavailability and plant response. Hydrothermal ZnO provides moderate improvements in germination, chlorophyll content, and yield due to its larger, less porous particles and slower zinc release, serving primarily as a basic micronutrient supplement. In contrast, curry leaf extract ZnO exhibits smaller, porous, flower-like nanostructures with bioactive phytochemical coatings, resulting in enhanced germination, root and shoot growth, photosynthetic activity, and higher biomass and fruit yield. This green-synthesized ZnO not only offers greater efficiency in nutrient delivery but also contributes to eco-friendly and sustainable agricultural practices, making it a superior option for improving tomato productivity and physiological performance.

## Reference

1. Bayda, S.; Adeel, M.; Tuccinardi, T.; Cordani, M.; Rizzolio, F. The History of Nanoscience and Nanotechnology: From Chemical–Physical Applications to Nanomedicine. Molecules 2020, 25, 112.
2. Mittal, D.; Kaur, G.; Singh, P.; Yadav, K.; Ali, S.A. Nanoparticle-Based Sustainable Agriculture and Food Science: Recent Advances and Future Outlook. Front. Nanotechnol. 2020, 2, 579954.
3. Gatoo, M.A.; Naseem, S.; Arfat, M.Y.; Dar, A.M.; Qasim, K.; Zubair, S. Physicochemical Properties of Nanomaterials: Implication in Associated Toxic Manifestations. Biomed Res. Int. 2014, 2014, 498420.
4. Liu, Y.; Mai, S.; Li, N.; Yiu, C.K.; Mao, J.; Pashley, D.H.; Tay, F.R. Differences between top-down and bottom-up approaches in mineralizing thick, partially demineralized collagen scaffolds. Acta Biomater. 2011, 7, 1742–1751.
5. Khan, I.; Saeed, K.; Khan, I. Nanoparticles: Properties, applications and toxicities. Arab. J. Chem. 2019, 12, 908–931.
6. Bhardwaj, B.; Singh, P.; Kumar, A.; Kumar, S.; Budhwar, V. Eco-Friendly Greener Synthesis of Nanoparticles. Adv. Pharm. Bull. 2020, 10, 566–576.
7. Mohamad, N.A.N.; Arham, N.A.; Jai, J.; Hadi, A. Plant extract as reducing agent in synthesis of metallic nanoparticles: A review. Adv. Mater. Res. 2013, 832, 350–355.
8. Logozzi, M.; Di Raimo, R.; Mizzoni, D.; Fais, S. The Potentiality of Plant-Derived Nanovesicles in Human Health-A Comparison with Human Exosomes and Artificial Nanoparticles. Int. J. Mol. Sci. 2022, 23, 4919.
9. Roy, A. Plant Derived Silver Nanoparticles and their Therapeutic Applications. Curr. Pharm. Biotechnol. 2021, 22, 1834–1847.
10. Vippola, M.; Valkonen, M.; Sarlin, E.; Honkanen, M.; Huttunen, H. Insight to Nanoparticle Size Analysis—Novel and Convenient Image Analysis Method versus Conventional Techniques. Nanoscale Res. Lett. 2016, 11, 169.
11. Simpson, D.S.A.; Oliver, P.L. ROS Generation in Microglia: Understanding Oxidative Stress and Inflammation in Neurodegenerative Disease. Antioxidants 2020, 9, 743.
12. Dröge, W. Free radicals in the physiological control of cell function. Physiol. Rev. 2002, 82, 47–95.
13. Forrester, S.J.; Kikuchi, D.S.; Hernandes, M.S.; Xu, Q.; Griendling, K.K. Reactive Oxygen Species in Metabolic and Inflammatory Signaling. Circ Res. 2018, 122, 877–902.
14. Alzoghaibi, M.A. Concepts of oxidative stress and antioxidant defense in Crohn's disease. World J. Gastroenterol. 2013, 19, 6540–6547.

15. Gilgun-Sherki, Y.; Melamed, E.; Offen, D. Oxidative stress induced-neurodegenerative diseases: The need for antioxidants that penetrate the blood brain barrier. Neuropharmacology 2001, 40, 959–975.
16. Rasheed, A.; Li, H.; Tahir, M.M.; Mahmood, A.; Nawaz, M.; Shah, A.N.; Aslam, M.T.; Negm, S.; Moustafa, M.; Hassan, M.U.; et al. The role of nanoparticles in plant biochemical, physiological, and molecular responses under drought stress: A review. Front. Plant Sci. 2022, 13, 976179.
17. Abdal Dayem, A.; Hossain, M.K.; Lee, S.B.; Kim, K.; Saha, S.K.; Yang, G.-M.; Choi, H.Y.; Cho, S.-G. The Role of Reactive Oxygen Species (ROS) in the Biological Activities of Metallic Nanoparticles. Int. J. Mol. Sci. 2017, 18, 120.
18. AshaRani, P.V.; Low, K.M.G.; Hande, M.P.; Valiyaveettil, S. Cytotoxicity and genotoxicity of silver nanoparticles in human cells. ACS Nano. 2009, 24, 279–290.
19. Carlson, C.; Hussain, S.M.; Schrand, A.M.; Braydich-Stolle, L.K.; Hess, K.L.J.R. Unique cellular interaction of silver nanoparticles: Size-dependent generation of reactive oxygen species. J. Phys. Chem. B. 2008, 112, 13608–13619.
20. Baig, N.; Kammakakam, I.; Falath, W. Nanomaterials: A review of synthesis methods, properties, recent progress, and challenges. Mater. Adv. 2021, 2, 1821–1871.
21. Nancharaiah, Y.V.; Mohan, S.V.; Lens, P.N.L. Biological and bioelectrochemical recovery of critical and scarce metals. Trends Biotechnol. 2016, 34, 137–155.
22. Jamkhande, P.G.; Ghule, N.W.; Bamer, A.H.; Kalaskar, M.G. Metal nanoparticles synthesis: An overview on methods of preparation, advantages and disadvantages, and applications. J. Drug. Deliv. Sci. Technol. 2019, 53, 101174.
23. Barhoum, A.; García-Betancourt, M.L.; Jeevanandam, J.; Hussien, E.A.; Mekkawy, S.A.; Mostafa, M.; Omran, M.M.; Abdalla, M.S.; Bechelany, M. Review on Natural, Incidental, Bioinspired, and Engineered Nanomaterials: History, Definitions, Classifications, Synthesis, Properties, Market, Toxicities, Risks, and Regulations. Nanomaterials 2022, 12, 177.
24. Jeevanandam, J.; Barhoum, A.; Chan, Y.S.; Dufresne, A.; Danquah, M.K. Review on nanoparticles and nanostructured materials: History, sources, toxicity and regulations. Beilstein J. Nanotechnol. 2018, 9, 1050–1074.
25. Shehzad, K.; Xu, Y.; Gaoc, C.; Duan, X. Three-dimensional macro-structures of two-dimensional nanomaterials. Chem. Soc. Rev. 2016, 45, 5541–5588.
26. Paras; Yadav, K.; Kumar, P.; Teja, D.R.; Chakraborty, S.; Chakraborty, M.; Mohapatra, S.S.; Sahoo, A.; Chou, M.M.C.; Liang, C.-T.; et al. A Review on Low-Dimensional Nanomaterials: Nanofabrication, Characterization and Applications. Nanomaterials 2023, 13, 160.
27. Kelly, K.L.; Coronado, E.; Zhao, L.L.; Schatz, G.C. The Optical Properties of Metal Nanoparticles: The Influence of Size, Shape, and Dielectric Environment. J. Phys. Chem. B 2003, 107, 668–677.
28. Yaqoob, A.A.; Ahmad, H.; Parveen, T.; Ahmad, A.; Oves, M.; Ismail, I.M.I.; Qari, H.A.; Umar, K.; Ibrahim, M.N.M. Recent Advances in Metal Decorated Nanomaterials and Their Various Biological Applications: A Review. Front. Chem. 2020, 8, 341.
29. Yaqoob, S.B.; Adnan, R.; Khan, R.M.R.; Rashid, R. Gold, Silver, and Palladium Nanoparticles: A Chemical Tool for Biomedical Applications. Front. Chem. 2020, 8, 376.
30. Chavali, M.S.; Nikolova, M.P. Metal oxide nanoparticles and their applications in nanotechnology. SN Appl. Sci. 2019, 1, 607. [Google Scholar] [CrossRef] [Green Version]

31. Huynh, K.-H.; Pham, X.-H.; Kim, J.; Lee, S.H.; Chang, H.; Rho, W.-Y.; Jun, B.-H. Synthesis, Properties, and Biological Applications of Metallic Alloy Nanoparticles. Int. J. Mol. Sci. 2020, 21, 5174.
32. Nguyen, T.K.; Thanh, N.M.; Mahiddine, S. Mechanisms of Nucleation and Growth of Nanoparticles in Solution. Chem. Rev. 2014, 114, 7610–7630.
33. Harish, V.; Ansari, M.M.; Tewari, D.; Gaur, M.; Yadav, A.B.; García-Betancourt, M.-L.; Abdel-Haleem, F.M.; Bechelany, M.; Barhoum, A. Nanoparticle and Nanostructure Synthesis and Controlled Growth Methods. Nanomaterials 2022, 12, 3226.
34. Ijaz, I.; Gilani, E.; Nazir, A.; Bukhari, A. Detail review on chemical, physical and green synthesis, classification, characterizations and applications of nanoparticles. Green Chem. Lett. Rev. 2020, 13, 223–245.
35. Thakkar, K.; Mhatre, S.S.; Parikh, R.Y. Biological synthesis of metallic nanoparticles. Nanomed. Nanomed.-Nanotechnol. 2010, 6, 257–262.
36. Dhand, C.; Dwivedi, N.; Loh, X.J.; Ying, A.N.J.; Verma, N.K.; Beuerman, R.W.; Lakshminarayanan, R.; Ramakrishna, S. Methods and strategies for the synthesis of diverse nanoparticles and their applications: A comprehensive overview. RSC Adv. 2015, 5, 105003–105037.
37. Abinaya, S.; Kavitha, H.P.; Prakash, M.; Muthukrishnaraj, A. Green synthesis of magnesium oxide nanoparticles and its applications: A review. Sustain. Chem. Pharm. 2021, 19, 100368.
38. Singh, J.; Dutta, T.; Kim, K.-H.; Rawat, M.; Samddar, P.; Kumar, P. Green' synthesis of metals and their oxide nanoparticles: Applications for environmental remediation. J. Nanobiotechnol. 2018, 16, 84.